Science Bulletin 65 (2020) 21–26

Contents lists available at ScienceDirect

Science Bulletin

journal homepage: www.elsevier.com/locate/scib

Article

Ferromagnetic tip induced unconventional superconductivity in Weyl semimetal

He Wang [a,b,c,1], Yingping He [a,d,1], Yiyuan Liu [a,d], Zhujun Yuan [a,d], Shuang Jia [a,d,e], Lei Ma [b,*], Xiong-Jun Liu [a,d,e,f,*], Jian Wang [a,d,e,f,*]

[a] International Center for Quantum Materials, School of Physics, Peking University, Beijing 100871, China
[b] Tianjin International Center for Nano Particles and Nano Systems, Tianjin University, Tianjin 300072, China
[c] Department of Physics, Capital Normal University, Beijing 100048, China
[d] Collaborative Innovation Center of Quantum Matter, Beijing 100871, China
[e] CAS Center for Excellence in Topological Quantum Computation, University of Chinese Academy of Sciences, Beijing 100190, China
[f] Beijing Academy of Quantum Information Sciences, Beijing 100193, China

ARTICLE INFO

Article history:
Received 10 September 2019
Received in revised form 21 October 2019
Accepted 31 October 2019
Available online 13 November 2019

Keywords:
Topological superconductivity
Coexistence of ferromagnetism and superconductivity
Weyl semimetal
Ferromagnetic tip-induced superconductivity
Point contact spectroscopy

ABSTRACT

The metallic tip-induced superconductivity in normal Weyl semimetal offers a promising platform to study topological superconductivity, which is currently a research focus in condensed matter physics. Here we experimentally uncover that unconventional superconductivity can be induced by hard point contact (PC) method of ferromagnetic tips in TaAs single crystals. The magneto-transport measurements of the ferromagnetic tip-induced superconducting (FTISC) states exhibit the quantum oscillations, which reveal that the superconductivity is induced in the topologically nontrivial Fermi surface of the Weyl semimetal, and show compatibility of ferromagnetism and induced superconductivity. We further measure the point contact spectra (PCS) of tunneling transport for FTISC states which are potentially of nontrivial topology. Considering that the magnetic Weyl semimetal with novel superconductivity is hard to realize in experiment, our results show a new route to investigate the unconventional superconductivity by combining the topological semimetal with ferromagnetism through hard PC method.

1. Introduction

Topological superconductor has attracted considerable attention in the fields of condensed matters physics and materials science [1–7], since it hosts Majorana bound states which have potential applications to the fault-tolerant quantum computation [8–10]. Recent discoveries of tip-induced unconventional superconductivity in non-superconducting topological semimetals, like single crystalline Dirac semimetal Cd_3As_2 [11] and Weyl semimetal TaAs single crystal [12], have made hard point contact (PC) method become a new approach to modulate and further detect the potential topological superconductivity [11–15]. In particular, the Weyl semimetal possesses pairs of Weyl points with definite chiralities and intrinsically topological Fermi surfaces [16–22], so the induced superconducting states in Weyl semimetals may inherit the topological nature from the parent compounds. However, when the time-reversal (TR) symmetry is not broken, the s-wave pairing may be favored and formed by TR partners, leading to the induced superconductivity with trivial topology in TaAs [23]. In comparison with the TR invariant Weyl semimetals, the Weyl semimetals with broken TR symmetry, e.g., due to magnetization, are highly promising materials in which the superconducting phases are widely predicted to be nontrivial [24–28]. Actually, unlike the conventional s-wave superconductivity, which is in general suppressed by the ferromagnetism [29], p-wave superconductivity can tolerate the ferromagnetic order [30,31]. In consequence, it is of great importance if the superconductivity can be induced in topological Weyl semimetal coexisting with ferromagnetism. Nevertheless, it is very challenging to experimentally realize intrinsic superconductivity in magnetic Weyl semimetal. So far there was no experimental report of superconducting phase coexisting with magnetism in semimetals.

2. Experimental

In this work, we report the induced superconductivity in the Weyl semimetal TaAs by using ferromagnetic tips (including nickel

* Corresponding authors.
E-mail addresses: jianwangphysics@pku.edu.cn (J. Wang), xiongjunliu@pku.edu.cn (X.-J. Liu), maleixinjiang@tju.edu.cn (L. Ma).
[1] These authors contributed equally to this work.

https://doi.org/10.1016/j.scib.2019.11.010

tip and cobalt tip) as a hard PC method. Point contacts were created by pressing a mechanically sharpened Ni (or Co) tip onto the (0 0 1) surface of TaAs single crystal, which was mounted on an Attocube nanopositioner stack. By inserting the stacks into a dry dilution refrigerator from Leiden with three-axis superconducting vector magnets, the temperature of sample can be as low as 0.3 K, and the applied maximum field in $X/Y/Z$ direction can be up to 1/1/3 T, respectively. Unlike the intrinsic magnetic Weyl semimetal, in our situation the ferromagnetic tips introduce the magnetism into the Weyl semimetal and break the TR symmetry. For the first time, the coexistence of unconventional superconductivity, ferromagnetism and topological non-trivial quantum oscillations in topological semimetals are systematically studied. Here, the ferromagnetic tip can also be taken as a selector of superconducting paring symmetry and offers strong evidence for topological non-trivial properties.

3. Results

A hard PC experiment is designed to induce superconductivity on (0 0 1) surface of Weyl semimetal TaAs single crystals in cryogenic PC system (related PC configuration can be referred to the inset of Fig. 1a). The major observations are below. (i) The quantum oscillations are observed in the ferromagnetic tip-induced superconducting (FTISC) states, and reveal that topologically nontrivial property remains under the tip. (ii) The compatibility of superconductivity and ferromagnetism suggests that the induced superconductivity can be potentially of p-wave type. In particular, the nearly 40 FTISC states have been detected and 11 of them have the PCS of double conductance peaks with double conductance dips, which are considered as typical spectral feature of a p-wave superconductor.

For one typical FTISC state with the PCS of double conductance peaks with double conductance dips obtained in Ni/TaAs PC experiment, the PC resistance as a function of temperature is shown in Fig. 1a. At 4.3 K the zero-field resistance drop in the blue curve is usually taken as a signature of superconducting transition. This transition point corresponds to the value of T_c, which vanishes when the perpendicular magnetic field ($H_{\perp}$) of 3 T is applied. Fig. 1b and c show the normalized PCS with conductance enhancement at low bias voltage correspondingly. This conductance enhancement can be further suppressed by increasing temperature or applying magnetic field, which again indicates the existence of superconductivity. Therefore, all the experimental data support that the FTISC state has been realized at or near the interface of the PC due to the lack of superconductivity in either Ni or TaAs single crystal.

The PCS shown in Fig. 1b and c can be caused by several possible mechanisms in our configuration. As the typical superconducting features in the PCS due to Andreev reflection at the interface of S/N junction [32], the double conductance peaks are usually observed at the temperature far below the T_c. For the p-wave superconductor, the double conductance peaks in PCS can be observed in either the PC experiment [33] or the planar junction [34]. One tunneling feature of latter work is two conductance dips at finite bias voltage, which is close to the superconducting gap value. In our PC configuration, the potential barrier at the contact

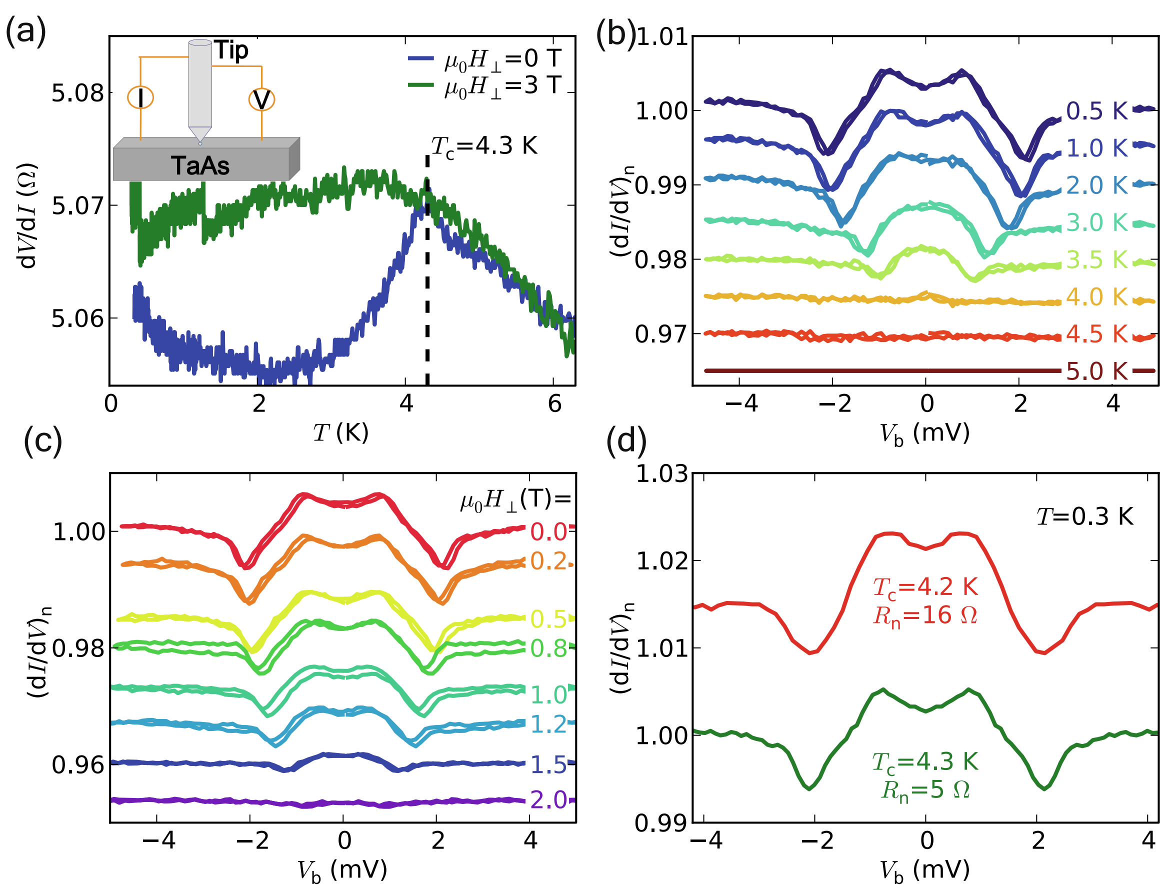

Fig. 1. The Ni/TaAs PC measurements of FTISC state of 5 Ω. (a) The temperature dependence of PC resistance at magnetic field of 0 T (blue), and 3 T (green), respectively. Inset: the schematics of the hard PC configuration in TaAs. (b) The corresponding normalized PCS at different temperatures without applying magnetic field. (c) The corresponding normalized PCS at different out-of-plane magnetic fields with the sample temperature of 0.3 K. (d) Two PCS of FTISC states with different PC resistance. The curves in this figure are shifted for clarity.

interface may arise from the degradation or contamination of the sample surface, as well as the mismatch of Fermi velocities between the TaAs and Ni tips. In special, even the contact interface is ideally clean, the mismatch of Fermi velocities of Ni/TaAs PC can still make the effective barrier parameter Z_{eff} larger than 1.4 (detailed calculation can be referred to the Supplementary Note 1). Thus, the tunneling scenario is suitable for our situation. On the other hand, the critical current effect [35] or the occurrence of multi-gaps [36] can also contribute double conductance dips in the PCS. In double-gap scenario, the conductance dip usually locates between two conductance peaks, which correspond to the energy values of two superconducting gaps. When increasing temperature or applying external magnetic field, this dip would disappear at $T< T_c$ or $H< H_{c2}$ [36]. But there is no extra peak feature out of the energy of the dip in Fig. 1b and c, and the conductance dips exist until the superconductivity is totally suppressed by increasing temperature or magnetic field. Thus, the condition of multi-gaps seems unlikely. Moreover, as shown in Fig. 1d, two FTISC states have similar T_c (4.2 K for 16 Ω state and 4.3 K for 5 Ω state). Although their PC resistance values are totally different, the conductance peaks and dips in their PCS locate at the same excitation energy values. This is inconsistent with the scenario of critical current effect, which shows normal state resistance dependence of the bias voltage of the conductance dip [35]. Considering the superconducting states either in present work or in the previous work [12] have double conductance peak and double conductance dips as the main feature of the PCS, it is natural to expect the feature of double conductance peaks with double conductance dips is intrinsic for FTISC state.

We have detected 11 FTISC states with similar PCS as shown in Fig. 1. Typical values of zero bias normal states resistance for stable contacts range from 2.3 to 27.8 Ω, and corresponding T_c from 4.2 to 6 K. Compared with the results of previous work with PtIr tip [12], it is important to be noted here: the highest T_c of FTISC states (6 K) is close to that of the previous one (~5.9 K) [12]. This indicates that the induced superconductivity is not suppressed by the ferromagnetic tips and thus is very likely to be spin triplet type, which could sustain in the case of TR symmetry broken.

The topological property of the FTISC states is proved by the measured so-called Shubnikov de Haas Oscillations (SdHOs) of the sample [37,38]. For the 5 Ω FTISC state, when the perpendicular magnetic field is up to 3 T, the typical feature of SdHOs is successfully observed in measured magnetoresistance (MR) curves at both 0.3 and 5.0 K (see Fig. S1 online). The SdHOs shown in Fig. 2a is obtained by subtracting a polynomial background from the original data at 0.3 K and shows the major frequency $F = 9.02$ T through Fourier transformation (to see the insets in Fig. 2a). Based on the Onsager formula $F = (\Phi_0/2\pi^2)S_F$ [39], where Φ_0 is the flux quantum with the value of $2.067833636 \times 10^{-15}$ Wb, we estimate the cross-sectional area of the Fermi surface $S_F = 8.61 \times 10^{-4}$ Å^{-2}, only taking about 2.573×10^{-2}% of total area of the first Brillouin zone in the k_x-k_y plane. It is consistent with the semi-metallic nature of TaAs, which intrinsically only possesses small Fermi pockets around Weyl points [16–22]. The Landau fan diagram is constructed by choosing the MR peak positions as the integer index and the dip positions as the half integer index [22]. The measured correlation between the Landau index and $1/B$ with linear extrapolation intercepting around zero is plotted in Fig. 2a, which is also a strong evidence of nontrivial π Berry phase associated Weyl fermions [38]. All these above experimental results clearly suggest that the typical topological nature of Weyl semimetal from TaAs single crystal is not changed for the FTISC states. On the other hand, the MR measurements also offer an opportunity to calculate the Fermi energy and the cyclotron mass of electrons in the FTISC states. Considering the influence of spin polarization on the p-wave type PCS, the superconducting gap shown in Fig. 1 can be estimated as 2.5 meV. Combining this gap value and the results of SdHOs, the Fermi energy of the corresponding FTISC state can be further estimated as 18 meV (details to see Supplementary Note 2), implying the Fermi level is much close to the Weyl point. In addition, the corresponding cyclotron mass of electrons is about 0.116 m_0, where the m_0 is the static mass of electron with the value of 9.1×10^{-31} kg. The estimated value of cyclotron mass of electron is consistent with previous result in TaAs [40], indicating the p-wave superconductivity scenario is valid to the detected FTISC states.

To further explore the influence of the ferromagnetic Ni tip on the induced superconducting states, we systematically measure the MR curves of the PC state (see Fig. 2b). In a small sweeping range of magnetic field, the hysteresis is observed; and the measured hysteresis of such system actually keeps almost same featured structure at both $T > T_c$ and $T < T_c$ (T_c is 4.3 K). When superconductivity is triggered in Ni/TaAs PC, especially the materials formed the PC are non-superconducting, the contribution of the spin-polarized electrons from the ferromagnetic tip to the superconducting states must be taken into consideration. Previous experimental and theoretical studies on the coexistence of superconductivity and ferromagnetism suggest that Cooper pairs can be formed by the spin-polarized electrons, which supports the spin-triplet state, especially p-wave superconductivity [31,41].

We also investigate the other 29 FTISC states, in which the mainly curve feature for their PCS is zero bias conductance hump

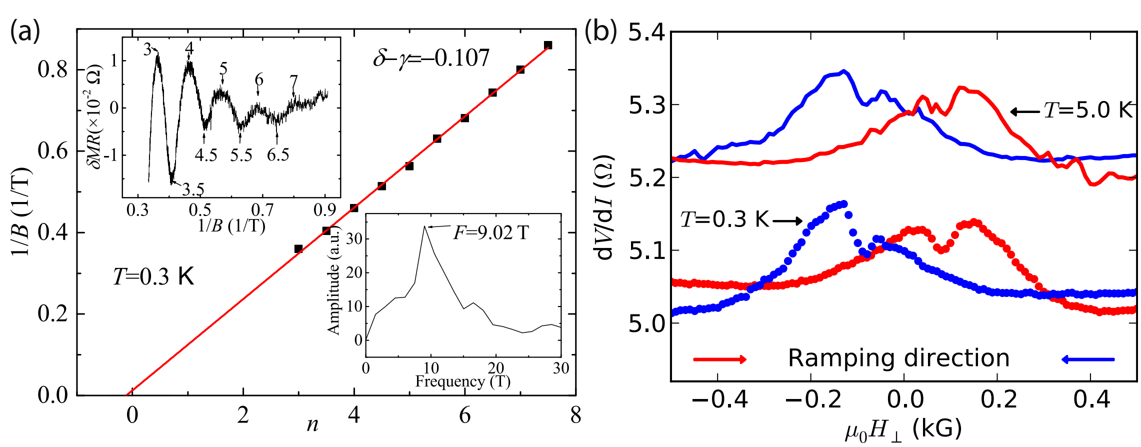

Fig. 2. The magneto-transport of FTISC state of 5 Ω. (a) The linear fitting of the Landau fan diagram with intercepts of –0.107. Upper inset: SdHOs after subtracting the background from raw data at 0.3 K. Lower inset: Fourier transformation of the oscillations showing a peak at 9.02 T. (b) The hysteretic MR of FTISC state in low perpendicular field regime.

(ZBCH). The results of one representative FTISC state of 3.57 Ω are shown in Fig. 3. According to the *R*-*T* curves (inset of Fig. 3a), the T_c is around 1 K, which is totally suppressed under the perpendicular magnetic field of 3 T. The corresponding PCS at different *T* and $H_\perp$ values at 0.3 K are presented in Fig. 3a and b, respectively. It can be seen that the spectral feature of ZBCH is further suppressed by either increasing *T* or applying $H_\perp$. This is reminiscent of the characteristic spectrum for superconducting PC states in thermal regime, which occurs when the contact size is larger than the mean free path of sample. It is important to address that the ZBCH can also be contributed by Andreev bound states, for which the energy scale of the ZBCH is close to the superconducting gap. This scenario is inconsistent with our results, as shown in Fig. S2 (online). Even the T_c values of two FTISC states are similar, the ZBCHs do not have same energy scale. Since the lack of split peak in the PCS under the magnetic field, the possibility of Kondo effect seems unlikely either. Hence, we believe that the thermal effect might be involved in our PCS with the feature of ZBCH.

Fig. 3c shows the observed SdHOs, for which the linear fitting of Landau index with respect to $1/B$ intercepts around zero, suggesting the possession of topological nontrivial nature in such FTISC states. The MR measurements show the hysteresis in MR curves, which survives at both $T > T_c$ and $T < T_c$ (T_c = 1 K, see Fig. 3d), indicating the compatibility between ferromagnetism and the induced-superconductivity in such a system. The magnetization switching field of 0.08 kG is close to the previous results [42], in which the switching field of Ni nanowire is about 0.1 kG at 10 K. Two kinds of PCS under the Ni tips are also obtained by using Co tips (see Fig. S3 online).

4. Discussion and conclusion

The experimental observation shows that the induced superconductivity coexists with the magnetization. This feature suggests that the tip-induced superconductivity might be p-wave type, as being proposed in our previous work, where a p-wave topological superconductor with TR and mirror symmetry was considered to interpret the experimental results [12]. Interestingly, we show here that while the magnetization may break both the TR and mirror symmetries, the Majorana surface modes in the proposed topological superconducting model are robust, which could potentially interpret the present new observation. In terms of Nambu basis: $\hat{c}_{\boldsymbol{k}}=(c_{k\uparrow}, c_{k\downarrow}, c^\dagger_{-k\uparrow}, c^\dagger_{-k\downarrow})$, with $c_{k,\sigma}=(c_{k,\sigma,a}, c_{k,\sigma,b})$ defined for a and b orbitals, the minimal model Hamiltonian is given by

$$H = (H_0 + M_x s_x + M_z s_z)\tau_z + \triangle \sin k_y \tau_y + M_y s_y, \quad (1)$$

$$\begin{aligned} H_0 = {} & \left[m_z + 2A(3 - \cos k_0 \cos k_x - \cos k_y - \cos k_z) - \mu\right]\sigma_z \\ & + 2B \sin k_0 \cos k_x \sigma_x + 2A \sin k_0 \sin k_x \sigma_z s_y + 2B \sin k_0 \cos k_x \sigma_z \\ & + 2B \cos k_0 \sin k_x \sigma_x s_y + 2B \sin k_z \sigma_y, \end{aligned} \quad (2)$$

where σ_i, s_i, and τ_i denote Pauli matrices acting on orbital, spin, and Nambu spaces, respectively, and the magnetization $M = (M_x, M_y, M_z)$. The system parameters *A*, *B*, m_z, and k_0 are taken as $A = B = 1$, $m_z = -2$; $k_0 = -1$ for convenience. Without magnetization, i.e., $M = 0$, the Hamiltonian *H* preserves the TR symmetry and mirror symmetry, respectively denoted by $T = \mathrm{i}s_y K$ and $M_y = \mathrm{i}s_y \tau_z$ [12]. In the (0 0 1) surface, the present WSM possesses helical gapless Fermi arc states protected by TR symmetry. The pairing term $\triangle \sin k_y$ gaps

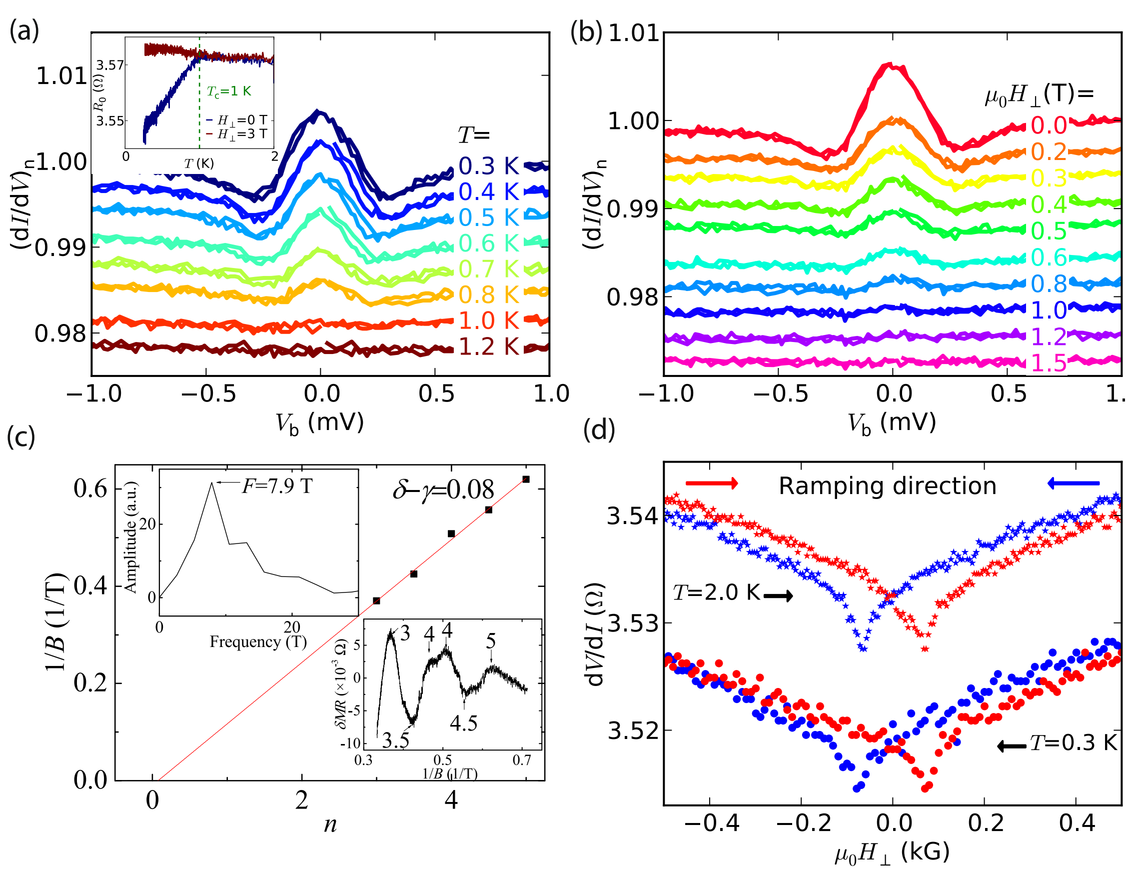

Fig. 3. The Ni/TaAs PC measurement of 3.53 Ω FTISC state showing ZBCH in PCS. (a) The normalized PCS at different *T*. Inset: the temperature dependence of PC resistance. The superconducting transition vanishes when the magnetic field of 3 T is applied in the perpendicular direction. (b) The normalized PCS at different perpendicular magnetic field. The curves in (a) and (b) are shifted for clarity. (c) The linear fitting of the Landau fan diagram with intercepts of 0.08. Upper inset: Fourier transformation of the oscillations showing peak at 7.9 T. Lower inset: SdHOs after subtracting the background from raw data at 0.3 K. (d) The hysteretic MR behavior in the perpendicular field at 0.3 and 2.0 K. The curves at 2 K have been shifted for clarity.

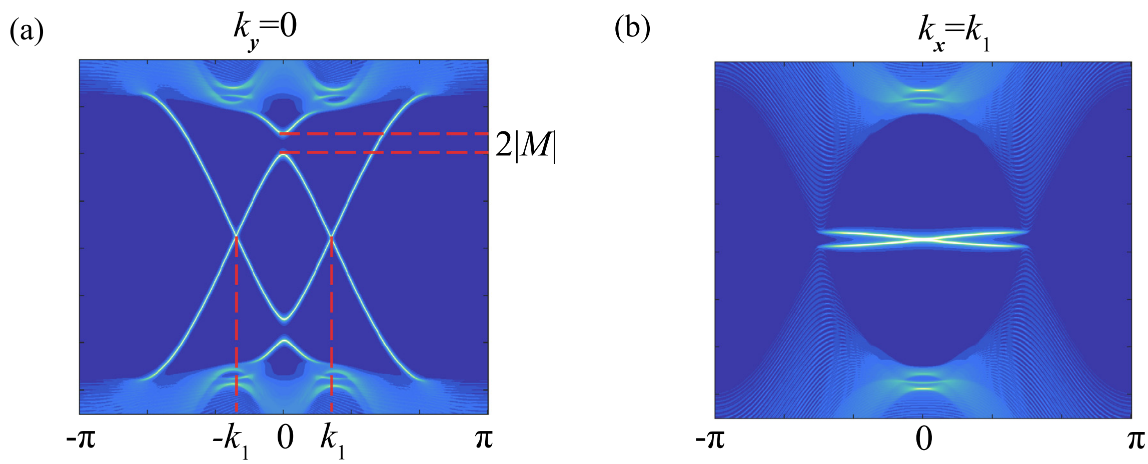

Fig. 4. Energy spectra of the bulk and surface states (a) along k_x direction; (b) along k_y direction with the magnetization $|\boldsymbol{M}| = 1.5\triangle$, $\theta = 10°$, where θ denotes the angle between the magnetization $\boldsymbol{M}$ and z axis. In our simulation, magnetization with large z-component and small in-plane component is considered. The magnetization breaks TR symmetry and opens a gap at the energy crossings of the helical arc states. Yet zero energy Majorana modes are preserved even in the presence of magnetization. All the numerical simulations are given with $\triangle$ equal to 0.05 times the hopping energy.

out the Fermi arc surface states along y direction except at $k_y = 0$ where the pairing potential vanishes. The surface states form two anisotropic Majorana cones at the $(k_x, k_y) = (\pm k_1, 0)$, with the dispersion along x direction inherited from the Fermi arc states and that along y direction determined by the pairing order [12].

The ferromagnetic Ni/Co tip induces magnetization mostly along z axis into TaAs (perpendicular to the (0 0 1) surface). With the magnetization energy being much smaller than the saddle point energy, the Weyl points cannot be annihilated by the magnetization. This is also verified by our SdHOs measurements which show a strong evidence of π Berry phase, indicating that the nontrivial topology of Weyl fermion is not damaged by the tip-induced magnetization. On the other hand, the magnetization breaks TRS and opens a gap at time reversal momentum $(k_x, k_y) = (0, 0)$, as verified by the numerical results in Fig. 4a. Further, unless the magnetization is along y direction, the Zeeman coupling also breaks the mirror symmetry. However, as shown in Fig. 4a and b, the zero-energy Majorana cone surface states are robust against magnetization. This is because a Majorana cone consists of the particles with spin in $+y$ direction and the holes with spin in $-y$ direction, respectively, while the magnetization couples only the opposite spin states of a particle (or hole). Thus the two Majorana cones at zero energy (Fermi energy) are changed by magnetization. Since the gap opening at $k_x = k_y = 0$ is far away from the zero energy, the Majorana modes in the superconducting gap are not affected (to see Fig. 4b). In consequence the main features of PC tunneling spectra could be unaffected by the ferromagnetic tip used in the experiment.

In order to test the reproducibility of these observations, up to 135 PC positions on three different samples from same batch have been measured with different ferromagnetic tips, including more than 400 PC states. Among them, 40 PC states in 20 PC positions exhibit superconductivity. These results are summarized in the Table 1. According to Table 1, the Co tip is more difficult to induce the superconducting states than Ni tip on the same sample, implying the material of the tip is one key factor for determining the success rate of the FTISC states.

Table 1
The success rate of FTISC states for different samples and different ferromagnetic tips. The success rate is defined as the PC positions containing FTISC states over the total PC positions.

Sample	Co tip	Ni tip
Sample 1	1/25	8/15
Sample 2	–	2/30
Sample 3	2/40	7/25

In conclusion, we have observed the FTISC states in Weyl semimetal TaAs for the first time. Typical p-wave PCS are observed in some FTISC states. Related MR measurements show that the topologically nontrivial nature under the tip maintains for the FTISC states and the induced superconductivity coexists with the ferromagnetism. Our observation suggests that the induced superconductivity in TaAs is unconventional and may potentially have nontrivial topology, which is further supported by our theoretical model.

Conflict of interest

The authors declare that they have no conflict of interest.

Acknowledgments

We thank Huichao Wang, Yanan Li and Jiawei Luo for the discussion on the experimental results. This work was financially supported by the National Key R&D Program of China (2018YFA0305604, 2017YFA0303302, and 2016YFA0301604), the National Natural Science Foundation of China (11888101, 11774008, 0401210001, 11574008, 11761161003, 11825401, 11704279, 11774255, U1832214, and 11774007), the Strategic Priority Research Program of Chinese Academy of Sciences (XDB28000000), the Beijing Natural Science Foundation (Z180010), the Key Project of Natural Science Foundation of Tianjin City (17JCZDJC30100), and China Postdoctoral Science Foundation (0401130005).

Author contributions

Jian Wang and Lei Ma conceived the experiments. He Wang carried out transport measurements under the instruction of Jian Wang. Yingping He and Xiong-Jun Liu performed the theoretical interpretation. Yiyuan Liu, Zhujun Yuan and Shuang Jia grew the crystals. He Wang and Jian Wang wrote the manuscript with the assistance of Xiong-Jun Liu and the input from other authors.

Appendix A. Supplementary materials

Supplementary materials to this article can be found online at https://doi.org/10.1016/j.scib.2019.11.010.

References

[1] Read N, Green D. Paired states of fermions in two dimensions with breaking of parity and time-reversal symmetries and the fractional quantum Hall effect. Phys Rev B 2000;61:10267.
[2] Kitaev AY. Unpaired Majorana fermions in quantum wires. Phys Usp 2001;44:131–6.
[3] Ivanov DA. Non-Abelian statistics of half-quantum vortices in p-wave superconductors. Phys Rev Lett 2001;86:268–71.
[4] Hasan MZ, Kane CL. Colloquium: topological insulators. Rev Mod Phys 2010;82:3045–67.
[5] Qi XL, Zhang SC. Topological insulators and superconductors. Rev Mod Phys 2011;83:1057–110.
[6] Fu L, Kane CL. Superconducting proximity effect and Majorana fermions at the surface of a topological insulator. Phys Rev Lett 2008;100:096407.
[7] Alicea J. New directions in the pursuit of Majorana fermions in solid state systems. Rep Prog Phys 2012;75:076501.
[8] Nayak C, Simon SH, Stern A, et al. Non-Abelian anyons and topological quantum computation. Rev Mod Phys 2008;80:1083–159.
[9] Alicea J, Oreg Y, Refael G, et al. Non-Abelian statistics and topological quantum information processing in 1D wire networks. Nat Phys 2011;7:412–7.
[10] Liu XJ, Wong CLM, Law KT. Non-Abelian Majorana doublets in time-reversal-invariant topological superconductors. Phys Rev X 2014;4:021018.
[11] Wang H, Wang HC, Liu HW, et al. Observation of superconductivity induced by a point contact on 3D Dirac semimetal Cd_3As_2 crystals. Nat Mater 2016;15:38–42.
[12] Wang H, Wang HC, Chen YQ, et al. Discovery of tip induced unconventional superconductivity on Weyl semimetal. Sci Bull 2017;62:425–30.
[13] Xing Y, Wang H, Li CK, et al. Superconductivity in topologically nontrivial material Au_2Pb. npj Quantum Mater 2016;1:16005.
[14] Wang H, Ma L, Wang J. Tip-induced or enhanced superconductivity: a way to detect topological superconductivity. Sci Bull 2018;63:1141–58.
[15] Wang J. Superconductivity in topological semimetals. Natl Sci Rev 2019;6:199–202.
[16] Weng H, Fang C, Fang Z, et al. Weyl semimetal phase in noncentrosymmetric transition-metal monophosphides. Phys Rev X 2015;5:011029.
[17] Huang SM, Xu SY, Belopolski I, et al. A Weyl fermion semimetal with surface Fermi arcs in the transition metal monopnictide TaAs class. Nat Commun 2015;6:7373.
[18] Xu SY, Beloposki I, Alidoust N, et al. Discovery of a Weyl fermion semimetal and topological Fermi arcs. Science 2015;349:613–7.
[19] Lv BQ, Weng HM, Fu BB, et al. Experimental discovery of Weyl semimetal TaAs. Phys Rev X 2015;5:031013.
[20] Lv BQ, Xu N, Weng HM, et al. Observation of Weyl nodes in TaAs. Nat Phys 2015;11:724–7.
[21] Zhang CL, Xu SY, Belopolski I, et al. Signatures of the Adler–Bell–Jackiw chiral anomaly in a Weyl fermion semimetal. Nat Commun 2016;7:10735.
[22] Huang XC, Zhao LX, Long YJ, et al. Observation of the chiral-anomaly-induced negative magnetoresistance in 3D Weyl semimetal TaAs. Phys Rev X 2015;5:031023.
[23] Aggarwal L, Gayen S, Das S, et al. Mesoscopic superconductivity and high spin polarization coexisting at metallic point contacts on Weyl semimetal TaAs. Nat Commun 2017;8:13974.
[24] Cho GY, Bardarson JH, Lu YM, et al. Superconductivity of doped Weyl semimetals: finite-momentum pairing and electronic analog of the 3He-*A* phase. Phys Rev B 2012;86:214514.
[25] Wei H, Chao SP, Aji V. Odd-parity superconductivity in Weyl semimetals. Phys Rev B 2014;89:014506.
[26] Bednik G, Zyuzin AA, Burkov AA. Superconductivity in Weyl metals. Phys Rev B 2015;92:035153.
[27] Zhou T, Gao Y, Wang ZD. Superconductivity in doped inversion-symmetric Weyl semimetals. Phys Rev B 2016;93:094517.
[28] Chan C, Liu XJ. Non-Abelian Majorana modes protected by an emergent second Chern number. Phys Rev Lett 2017;118:207002.
[29] Shen R, Zheng ZM, Liu S, et al. Breakdown of the coexistence of spin-singlet superconductivity and itinerant ferromagnetism. Phys Rev B 2003;67:024514.
[30] Rice TM, Sigrist M. Sr_2RuO_4: an electronic analogue of ^{3}He? J Phys Condens Matter 1995;7:L643–8.
[31] Fay D, Appel J. Coexistence of p-state superconductivity and itinerant ferromagnetism. Phys Rev B 1980;22:7.
[32] Blonder GE, Tinkham M, Klapwijk TM. Transition from metallic to tunneling regimes in superconducting microconstrictions: excess current, charge imbalance, and supercurrent conversion. Phys Rev B 1982;25:4515.
[33] Laube F, Goll G, Hv Löhneysen, et al. Spin-triplet superconductivity in Sr_2RuO_4 probed by Andreev reflection. Phys Rev Lett 2000;84:1595.
[34] Kashiwaya S, Kashiwaya H, Saitoh K, et al. Edge states of Sr_2RuO_4 detected by in-plane tunneling spectroscopy. Phys Rev Lett 2011;107:077003.
[35] Sheet G, Mukhopadhyay S, Raychaudhuri P. Role of critical current on the point-contact Andreev reflection spectra between a normal metal and a superconductor. Phys Rev B 2004;69:134507.
[36] Daghero D, Gonnelli RS. Probing multiband superconductivity by point-contact spectroscopy. Supercond Sci Technol 2010;23:043001.
[37] Shoenberg D. Magnetic oscillations in metals. Cambridge, England: Cambridge University Press; 1984.
[38] Wang CM, Lu HZ, Shen SQ. Anomalous phase shift of quantum oscillations in 3D topological semimetals. Phys Rev Lett 2016;117:077201.
[39] Mikitik GP, Sharlai YV. Manifestation of Berry's phase in metal physics. Phys Rev Lett 1999;82:2147.
[40] Arnold F, Naumann M, Wu SC, et al. Chiral Weyl pockets and Fermi surface topology of the Weyl semimetal TaAs. Phys Rev Lett 2016;117:146401.
[41] Aoki D, Huxley A, Ressouche E, et al. Coexistence of superconductivity and ferromagnetism in URhGe. Nature 2001;413:613.
[42] Rheem Y, Yoo B-Y, Beyermann WP, et al. Magnetotransport studies of a single nickel nanowire. Nanotechnology 2006;18:1.

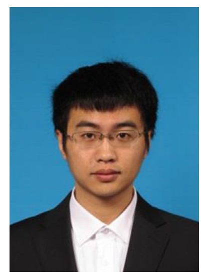

He Wang received his B.S. degree from Tianjin University in 2007 and Ph.D. degree in 2016 from Peking University. He was a postdoc at Tianjin international center of nano-particle and nano-system in Tianjin University from 2016 to 2018. He is now a faculty at Department of Physics in Capital Normal University. His research mainly focuses on the physical properties of unconventional superconductor.

Lei Ma earned his Ph.D. degree in 2010. Then he had his Postdoc training in Brown University and Georgia Tech. From 2016, he took a full professor position in Tianjin University as a Beiyang outstanding oversea scholar and Tianjin 1000 Talent youth scholar. His research mainly focuses on graphene electronics related physics and cluster physics as well as the instrumentation of mass spectrometer and high resolution photo-electrometer.

Xiong-Jun Liu received his Ph.D. degree in Texas A&M University in 2011, and was a postdoctoral fellow in University of Maryland, IAS HKUST and MIT. He joined the faculty of ICQM, Peking University (09/2014), became tenured (07/2018) and now a full professor (from 01/2019). He works in condensed matter theory and ultracold atoms, focusing on quantum simulation and topological matter: topological superconductors, synthetic gauge fields, non-equilibrium topological quantum systems, and strongly correlated topological states.

Jian Wang received his B.S. degree from Shandong University in 2001 and Ph.D. degree from Institute of Physics, Chinese Academy of Sciences in 2007. He is now a Changjiang Distinguished Professor at International Center for Quantum Materials, School of Physics, Peking University. His current research interest is mainly focused on the physical properties of low dimensional superconductors and topological materials.